Deuteron magnetic resonance in tantalum, niobium, and vanadium deuterides

N. Salibi,* B. Ting,† D. Cornell,‡ and R. E. Norberg
Department of Physics, Washington University, St. Louis, Missouri 63130
(Received 19 January 1988)

Deuteron magnetic resonance has been used to measure line shapes and relaxation rates in a series of Ta, Nb, and V deuterides between 190 and 580 K. Results are compared with corresponding data in hydrides to reveal dipolar, quadrupolar, and electronic rate contributions in various phases. Korringa constants, diffusion activation energies, and the effects of magnetic and electric field inhomogeneities are examined. Deuteron relaxation associated with hopping among tetrahedral interstitial sites in α phases is primarily quadrupolar. In the warm portions of the β phase, the dominant relaxation is dipolar because the deuteron hopping occurs only among an ordered subset of interstitial sites. At lower temperatures quadrupolar relaxation again dominates, before decreasing around 200 K.

I. INTRODUCTION

Deuteron magnetic resonance (DMR) provides a useful perspective on the structure and dynamics of the transition metal and deuterides of Ta, Nb, and V. If there exist only small isotopic effects on this structure and dynamics then comparison with reported proton NMR results for corresponding hydrides permits identification of quadrupolar contributions to the DMR data and provides new information about deuteron motions and site occupancy. Seymour has reviewed[1] the limitations on such comparisons in previous studies. Even in bcc metal deuterides where the metal atoms produce electric field gradients at the D interstitial sites, electron screening can modify the anticipated proportionality between metal-generated quadrupolar and dipolar deuteron relaxations.

It is well known[1-3] that in β phase, rapid deuteron hopping on a superlattice of ordered interstitial sites does not average out the quadrupolar splitting of the rigid lattice DMR line shape. In the present work we show that such β-phase hopping among ordered sites also does not produce quadrupolar spin-lattice relaxation and the principal observed corresponding deuteron relaxation is dipolar. At lower temperatures, but still in the motional relaxation regime, quadrupolar relaxation reappears as site occupancies change.

Experimental results to be discussed include DMR line shapes and the relaxation rates $\Gamma_1(T_1^{-1})$, $\Gamma_2(T_2^{-1})$, and spin-lock $\Gamma_{1\rho}(T_{1\rho}^{-1})$. Throughout the present paper Kelvin temperatures are followed by the corresponding quantity $(10^3/T)$ in parentheses.

II. EXPERIMENTAL PROCEDURE

Pulsed DMR measurements were made at 7.55 and 30.7 MHz using a 12-kG electromagnet-based spectrometer and a 47-kG CXP200. Sample temperatures were controlled between 150 and 580 K by flow cryostats using heated-air or cooled-nitrogen gas.

The metal deuteride samples investigated were provided by R. G. Barnes and were those previously examined by Roenker.[2] Vanadium and tantalum metal powders were deuterided by the Metallurgy Division of Ames Laboratory using highly purified deuterium gas. Niobium deuterides were purchased from the Ventron Corporation. The samples consisted of 325 mesh powders with impurity contents given by Roenker.[2]

The deuteron spin-lattice relaxation rates Γ_1 in the laboratory frame were measured using a $180°$-τ-$90°$ pulse sequence and/or an inversion recovery quadrupole echo (IRQE) sequence. The transverse relaxation rates Γ_2 were determined from line shapes and from two-pulse,[4] Carr-Purcell-Meiboom-Gill[5] (CPMG), and Wayne-Zamir-Strange[6] (WZS) pulse arrays. Spin-lattice relaxation rates $\Gamma_{1\rho}$ in the rotating frame were measured at 30.7 MHz with a spin-locking field H_1 of 9 G (and in a few cases, with lower H_1 fields).

III. RESULTS AND INTERPRETATION

A. Tantalum deuterides

Determinations of the phase diagram for TaH_x have been summarized by Schober and Wenzl.[7] Differential thermal analysis (DTA) measurements by Kobler and Schober[8] show that near H concentration 0.6 the α' phase solid solution in a somewhat expanded bcc metal lattice occurs above 325 K. At this composition there may exist an $(\alpha'+\epsilon')$ phase over a small interval near 320 K. Below 320 K the β phase occurs with ordered H occupancy of a superlattice of some of the interstitial sites. Below 297 K there occurs a $(\beta+\delta)$ mixed phase and below 253 K a $(\beta+\zeta)$ structure.

It is anticipated[7] that the TaD_x phase diagram should be similar to that for TaH_x, but some modest differences have been reported. For $TaD_{0.60}$ the phase diagram determined primarily from DMR by Slotfeldt-Ellingsen and Pedersen[3] shows additional transitions $\alpha \rightarrow \alpha''$ near 349 K and $\alpha'' \rightarrow \alpha'+\beta'$ at 335 K. These results are somewhat controversial[7] and do not agree with the results reported by Asano, Ishino, Yamada, and Hirabayashi.[9] It will be shown that the present DMR results do indicate isotopic

differences between the TaH_x and TaD_x phase diagrams. The deuterium spin-lattice relaxation rate in the α-phase metal deuterides can be written as

$$\Gamma_1(\mathrm{D}) = \Gamma_{1e} + \Gamma_{1d} + \Gamma_{1q} . \quad (1)$$

Here Γ_{1e} is the rate arising from the conduction electrons, Γ_{1d} reflects dipolar interaction of ^{2}D with the metal nuclei (the D-D coupling being negligible), and Γ_{1q} is the relaxation rate arising from the coupling of the deuteron quadrupole moment with static electric field gradients which also arise primarily from the metal sites. The last two terms of Eq. (1) are sensitive to atomic diffusion and, for Arrhenius-governed deuteron diffusion, can be written

$$\Gamma_{1\,\mathrm{diff}} = \Gamma_0 e^{E_D/kT} . \quad (2)$$

Here E_D is the activation energy of deuteron diffusion and the metal atoms are assumed not to diffuse on the time scale of the interaction. It has been assumed that the deuteron dipolar and quadrupolar interactions both arise from the adjacent metal sites; that screening effects do not vary appreciably over the temperature range of the data; and that it is reasonable to neglect any different dependences[10] of dipolar and quadrupolar relaxation on diffusion. The experimental results will be shown to support these assumptions.

Equations (1) and (2) give

$$\Gamma_1(\mathrm{D}) = \frac{T}{C_D} + \Gamma_0 e^{E_D/kT} , \quad (3)$$

where C_D is the deuterium Korringa[11] constant. A weighted least-squares three-parameter fit to the experimental $\Gamma_1(\mathrm{D})$ data yields C_D, Γ_0, and E_D. Knowledge of C_D allows the determination of Γ_{1e}.

Proton and deuteron rates in corresponding hydrides and deuterides can be compared,[12] neglecting isotopic differences in phase diagrams and hopping rates. Assuming that the proton dipolar relaxation also is dominated by interaction with adjacent metal atoms, the dipolar D and H rates[13] scale as the square of the nuclear gyromagnetic ratios and so at high temperatures the dipolar Γ_1 rates are related by

$$\Gamma_{1d}(\mathrm{D}) = \frac{1}{42.44} e^{(E_D - E_H)/kT} \Gamma_{1d}(\mathrm{H}) . \quad (4)$$

E_D and E_H are the deuteron and proton diffusion activation energies in M-D and M-H, respectively. $\Gamma_{1d}(\mathrm{H})$ is the dipolar proton relaxation rate observed in hydrides. The quadrupolar contribution to $\Gamma_1(\mathrm{D})$ is then given by Eq. (1).

The deuteron quadrupolar and dipolar rates can be compared:

$$\Gamma_{1q}(\mathrm{D}) = \frac{2\pi^2 \nu_Q^2}{3A} \Gamma_{1d}(\mathrm{D}) . \quad (5)$$

Here ν_Q is the electric quadrupole coupling constant and

$$A = \tfrac{4}{3} \gamma_S^2 \gamma_I^2 \hbar^2 S(S+1) \sum_j r_j^{-6} ,$$

where S and I refer to the metal and deuterium nuclei, respectively, and the lattice sum involves the distances between unlike spins. Defining $B_{SD} = \gamma_S^2 \gamma_I^2 \hbar^2 S(S+1)$ the expression for A becomes

$$A = 195.33 B_{SD} b_0^{-6} ,$$

where b_0 is the bcc cube edge lattice parameter.

Relaxation data were taken in the α phase of four samples of TaD_x with $x = 0.43$, 0.50, 0.60, and 0.76. Figure 1 shows the α-phase 7.55 MHz relaxation rate $\Gamma_1(\mathrm{D}) = 1/T_1(\mathrm{D})$ in the sample with $x = 0.43$. The lines show deduced constituent rates Γ_{1q}, Γ_{1d}, and Γ_{1e}. The data and analyses are similar for $x = 0.50$, 0.60, and 0.76. At all concentrations the α-phase deuteron rate $\Gamma_1(\mathrm{D})$ decreases continuously as the temperature increases, indicating the conduction-electron contribution Γ_{1e} does not dominate the deuteron relaxation up to 580 K. In TaD_x the principal deuteron interstitial site occupancy is expected to be tetrahedral.

The proton relaxation rate $\Gamma_1(\mathrm{H})$ reported in tantalum hydrides by Mauger, Williams, and Cotts[14] shows that at 433 K $\Gamma_1(\mathrm{H})$ levels off ($x = 0.76$) or starts to increase ($x \leq 0.6$). Thus at higher temperatures the conduction-electron contribution to $\Gamma_1(\mathrm{H})$ in TaH_x is at least comparable to the α-phase dipolar contribution. Results of the three-parameter fit to $\Gamma_1(\mathrm{D})$ in α-TaD_x are presented in Table I. 30.7-MHz $\Gamma_1(\mathrm{D})$ results, to be discussed below, yield a somewhat larger apparent activation energy of 0.24 eV/atom for the $TaD_{0.60}$ sample.

The Korringa constant C_H for protons also has been reported.[14] If deuteride and hydride structures are the same C_D scales from C_H by a factor of 42.44 ($= \gamma_H^2/\gamma_D^2$). The scaled C_H values (open triangles) in Fig. 2 are in very good agreement with the values of C_D obtained in the present work (solid triangles). The increase of C with x has been observed in several M-H systems and in the present deuterides. The increase has been regarded as supportive evidence for the rigid-band model and the view

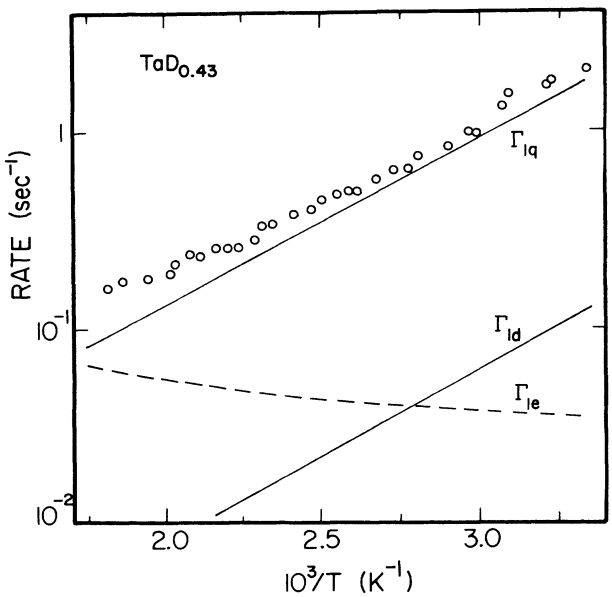

FIG. 1. Deuteron spin-lattice relaxation rates $\Gamma_1(\mathrm{D})$ in $TaD_{0.43}$. The solid lines indicate quadrupolar and dipolar contributions Γ_{1q} and Γ_{1d}. The dashed curve shows the electronic contribution Γ_{1e}.

TABLE I. Reduced data from α'-TaD_x.

D/Ta	E_D (eV/atom)	$T_{1e}T$ (10^4 sec K)
0.43	0.18 ± 0.02	0.9 ± 0.1
0.50	0.19 ± 0.02	1.0 ± 0.1
0.60	0.19 ± 0.02	1.4 ± 0.1
0.65[a]	0.22 ± 0.002	1.7 ± 0.2
0.76	0.21 ± 0.02	2.2 ± 0.2

[a]From Ref. 13.

that hydrogen (deuterium) atoms dissolved in a metal give up their electron to the conduction band. At higher ^1H (^2D) concentrations the density of states at the Fermi level $N(E_F)$ is reduced, thus decreasing the electronic relaxation rate which is proportional to $[N(E_F)]^2$. The increased C_H and C_D as ^1H and ^2D concentration increases implies the existence of a smaller electronic contribution to the relaxation rate at higher concentrations.

Diffusional activation energies E_H in TaH_x and E_D in α-phase TaD_x are plotted versus x in Fig. 3. The NMR determination of E_H by Mauger, Williams, and Cotts[14] gives results which are in good agreement with the Gorsky-effect measurements by Bauer *et al.*[15] Both sets of data show an increase in E_H up to 40% ^1H concentration. For higher x, E_H is approximately independent of concentration. The activation energy E_D in TaD_x (solid dots and triangles) has a variation with x that is similar to that of E_H. Bauer's data,[15] which go up to $x = 0.4$, show that E_D increases with concentration. Within experimental error, the activation energy in TaD_x for $x > 40\%$ is about 0.2 eV/atom. The concentration independence of E_H at high concentrations was also observed in NbH_x by Williams.[16] The difference between the activation energies of ^1H and ^2D reflects a difference in their zero-point

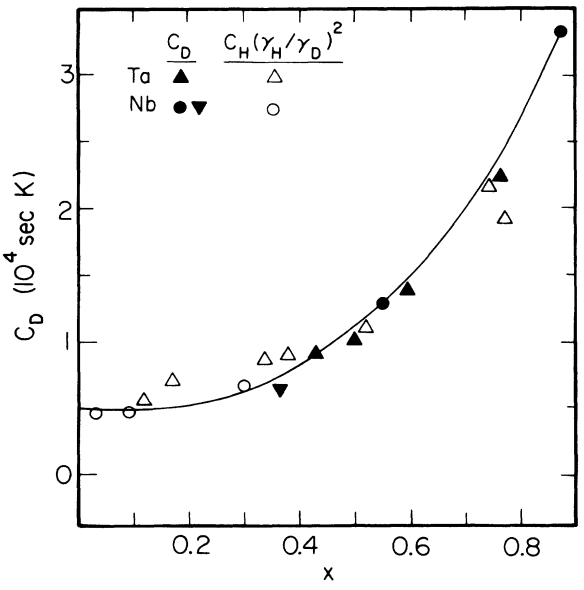

FIG. 2. Deuteron Korringa constants for TaD_x and NbD_x are indicated by solid symbols. The open symbols are proton results in corresponding hydrides, scaled by γ^2.

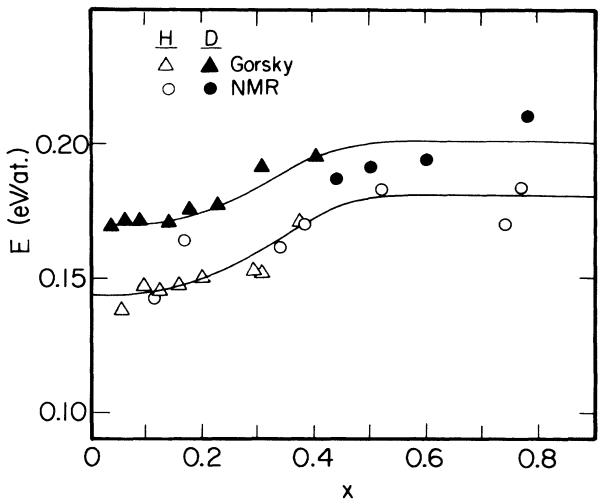

FIG. 3. Diffusional activation energies as a function of x in α-phase TaD_x and TaH_x. Gorsky effect measurements and NMR determinations are shown (Refs. 14–16).

energies.

With C_D, E_D, and E_H known, separate contributions to the relaxation can be extracted from the experimental rates $\Gamma_1(D)$ following Eqs. (1)–(5). The dipolar contribution is derived using Eq. (4) and the reported[14,17] spin-lattice relaxation rates of ^1H in the hydrides. Over the α-phase temperature range and concentrations studied (Fig. 1) the quadrupolar relaxation is dominant. Dipolar relaxation in α phase never exceeds a maximum of 7% of $\Gamma_1(D)$.

The electric quadrupole coupling constant ν_Q in α'-TaD_x can be derived from Γ_{1d}, Γ_{1q}, and Eq. (5). In $TaD_{0.43}$, $TaD_{0.50}$, and $TaD_{0.60}$, ν_Q is found to be 40 kHz and in $TaD_{0.76}$ 37 kHz. The variation lies within the error on ν_Q ($\sim 8\%$) and so ν_Q may be considered to be concentration independent and equal to 40 kHz in the α-TaD_x samples studied.

The few T_2 measurements reported in hydrides and deuterides have shown free-induction decay or two-pulse echo Γ_2 values that level off two or three orders of magnitude above Γ_1 in the motionally narrowed regime. This behavior reflects fast diffusion of the resonant nuclei in large magnetic field gradients associated with the bulk magnetic susceptibility of powdered samples. In the deuterides the quadrupolar interaction of the diffusing deuterons with spatially varying electric field gradients arising from dislocations and grain surfaces also contributes to the broadening to the linewidth.

Figure 4 shows Γ_2 and $\Gamma_1(D)$ rate measurements in $TaD_{0.43}$. The Γ_2 results include the spin echo-decay rates Γ_2 (solid dots). Corrected transverse rates Γ_{2t} (solid triangles) were obtained with Γ_2 measurements similar to those performed by Zamir and Cotts[18] on powdered NbH_x samples using series of CPMG sequences with different values of τ. The measured relaxation rate is

$$\Gamma_{2m} = \Gamma_{2t} + \tfrac{1}{3}\gamma^2 G^2 D \tau^2 . \quad (6)$$

Here Γ_{2t} is the true relaxation rate, γ the gyromagnetic ratio of the diffusing nuclei, G the gradient, D the

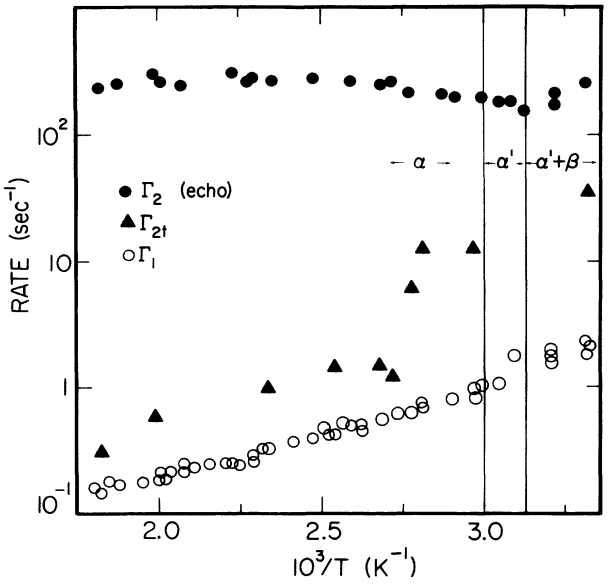

FIG. 4. Deuteron spin-lattice rates Γ_1(D) and transverse rates Γ_2(D) for $TaD_{0.43}$. The triangles indicate corrected Γ_{2t}(D) rates. The vertical lines indicate the reported (Ref. 3) transitions $\alpha \rightarrow \alpha' \rightarrow (\alpha'+\beta)$.

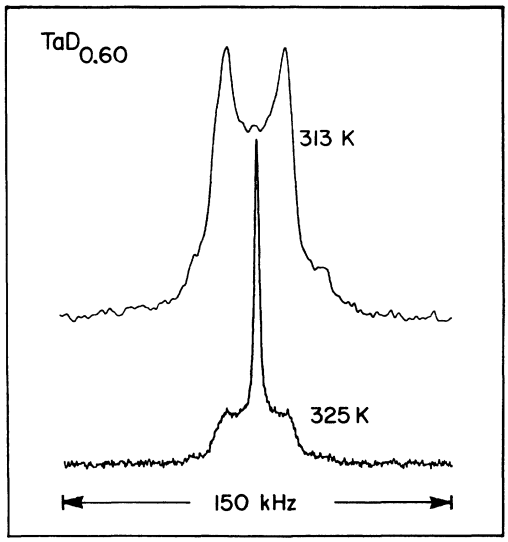

FIG. 5. DMR line shapes for $TaD_{0.60}$ in the $(\alpha'+\beta')$ and $(\epsilon+\beta)$ phases at 325 and 313 K. The β-phase quadrupole splitting corresponds to $\nu_Q = 43$ kHz. An anisotropic Knight shift distorts the spectra.

diffusion coefficient, and τ the pulse separation. The extrapolation of a plot of Γ_{2m} vs τ^2 to $\tau^2 = 0$ gives Γ_{2t}.

The corrected rate Γ_{2t} nearly is equal to Γ_1 between 555 K (1.80) and 364 K (2.75), where Γ_{2t} begins a sharp increase well above the reported[3] phase transition $\alpha \rightarrow \alpha'$. The Γ_{2t} increase reflects a reduction in the deuteron hopping rate since the quadrupole coupling frequency does not change much at the $\alpha \rightarrow \alpha''$ transition. The total rate Γ_2 itself shows a minimum in the vicinity of the phase transition. Similar minima occur in the Γ_2 results for $x = 0.76$, 0.60, and 0.50.

Figure 5 shows 30.7-MHz Fourier-transform DMR spectra in $TaD_{0.60}$ at two temperatures. The vertical arrows and reduced spectra at the bottom of Fig. 6 show the locations of these temperatures on a $10^3/T$ scale. At 325 K (3.08) [$\alpha'+\beta'$ region just above the transition to β] the spectrum displays the narrow α-phase component superimposed on an emergent β-phase doublet spectrum with a nearly resolved 43-kHz quadrupole coupling frequency.

The other spectrum in Fig. 5 is that at 313 K (3.19) in the β regime. The α-phase narrow central line has vanished and the principal spectral feature is a $\nu_q = 43$ kHz doublet associated with β phase. The line has an asymmetry parameter near 0.14 and is distorted by an anisotropic Knight shift.[19]

Figure 6 summarizes the DMR relaxation rates in $TaD_{0.60}$. Open circles show Γ_1(D) at 7.55 MHz. Open triangles and solid dots show Γ_1(D) at 30.7 MHz. The dots correspond to rates Γ_1(D) for the central α portion of the line and the triangles to rates for the wings of the line. The solid triangles show 30.7-MHz spin lock rates $\Gamma_{1\rho}$(D) at 9 G H_1. Γ_1(D) increases with decreasing temperature in α phase and the decomposition into Γ_{1d}, Γ_{1q}, and Γ_{1e} is similar to that shown for $TaD_{0.43}$ in Fig. 1. The solid curve in α phase shows the γ^2-scaled Γ_1(H) results of Mauger, Williams, and Cotts[14] (7 MHz) interpolated to $TaH_{0.60}$ and also those of Hornung[20] (40 MHz) for $TaH_{0.597}$. The Γ_1(H) rates have been divided by 42.44 to indicate Γ_{1e}(D)+Γ_{1d}(D). No frequency correction has been applied since no frequency dependence is observed in

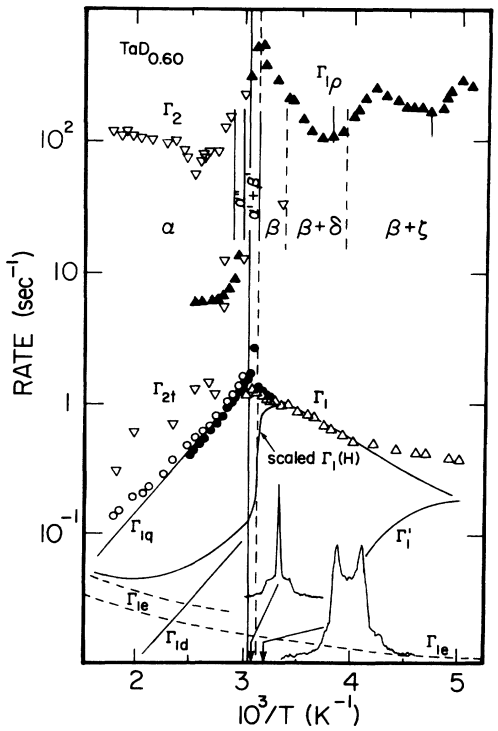

FIG. 6. Summary of DMR relaxation rates in $TaD_{0.60}$ between 200 and 565 K. The relaxation Γ_1(D) in α phase is primarily quadrupolar while that in β phase is dipolar. Arrows at the bottom indicate locations of the spectra from Fig. 5.

the α-phase DMR and the data are in the extreme narrowed regime. At high temperatures the solid curve nicely approaches our $\Gamma_{1e}(D)$ result (upper dashed curve) determined from the three-parameter fit to the 7.55 MHz $\Gamma_1(D)$ results. The lower dashed line shows a slightly different $\Gamma_{1e}(D)$ curve determined by γ^2 scaling of the $\Gamma_{1e}(H)$ results of Kazama and Fukai[21] for $TaH_{0.63}$. The sloping straight lines indicate $\Gamma_{1d}(D)$ and $\Gamma_{1q}(D)$ and correspond to $E_D = 0.19$ eV/atom.

The vertical lines in Fig. 6 indicate reported phase changes. The solid lines indicate those for $TaD_{0.60}$ and the dashed lines those for $TaH_{0.60}$. The long solid line indicates the 329 K (3.04) α to β_1 transition reported by Asano *et al.*[9] in $TaD_{0.60}$. The long dashed line shows the $(\alpha'+\epsilon)$ to β transition reported at 320 K (3.13) for $TaH_{0.60}$ by Kobler and Schober[8] and by Schober and Wenzl.[7] This also is the temperature of the $(\alpha'+\beta')$ to β transition (solid line segment) reported for $TaD_{0.60}$ by Slotfeldt-Ellingsen and Pedersen.[3] To the left the solid line segments indicate their reported α to α'' and α'' to $(\alpha'+\beta)$ transitions. To the right the dashed line segments indicate the reported[7,8] $TaH_{0.60}$ transitions β to $(\beta+\delta)$ and $(\beta+\delta)$ to $(\beta+\zeta)$. At the upper right the very short solid lines indicate the transitions $(\beta+\delta)$ to $(\beta+\theta)$ and $(\beta+\theta)$ to θ reported by Hornung, Khan, Torgeson, and Barnes.[22]

Below 323 K (3.10) the solid curve reflects Hornung's $\Gamma_1(H)$ results[20] scaled by 42.44 and by a linear frequency factor (40/30.7), on the presumption that the data here reflect proximity to a motional Γ_1 peak. The excellent agreement with the present $\Gamma_1(D)$ results (open triangles) indicates that β phase deuteron relaxation primarily is dipolar and that the deuteron hopping here is among an ordered subset of interstitial sites for which the site electric field gradients are the same in magnitude and orientation. In this same temperature interval (cf. the arrows and spectra in Fig. 6) the DMR line shapes of Fig. 5 show the appearance of the characteristic β-phase quadrupolar doublet spectra similarly unaveraged by the restricted deuteron hopping. In the $(\alpha'+\beta')$ mixed-phase regime at 325 K (3.08) an α-phase $\Gamma_1(D)$ relaxation rate component still is observed (solid circles in Fig. 6) for the central port of the line and increases to a factor of 2 larger than the rate for the broader β-phase components (triangles) as quadrupolar relaxation persists for the disordered α-phase hopping. The two-component $\Gamma_1(D)$ rates and the composite DMR spectra support the existence of the mixed $(\alpha'+\beta')$ phase, which has been controversial.[3,7,9]

At the transition away from α phase, $\Gamma_{1\rho}(D)$ increases dramatically (solid triangles) as does $\Gamma_{2l}(D)$ (inverted triangles and cf. Fig. 4) and also the dipolar $\Gamma_{1d}(D)$ rate (solid curve), which increases because the hopping rate decreases suddenly. $\Gamma_{1\rho}(D)$ at lower temperatures shows successive broad minima near the phase-transition temperatures (short vertical dashed lines) reported by Hornung, Khan, Torgeson, and Barnes[22] ($TaH_{0.597}$). It may be that the transitions are broadened and shifted by the presence of impurities. Clearly $\Gamma_{1\rho}(D)$ shows more sensitivity to the phase changes than does $\Gamma_1(D)$.

Near 250 K (4.00) a deviation begins to appear between the present $\Gamma_1(D)$ rates and the solid curve dipolar Γ_{1d} line scaled from the proton rates. The difference rate Γ_1' is shown as a short rising curve. It apparently reflects the reappearance of quadrupolar relaxation as hopping no longer is restricted to the β-phase ordered subset of sites. In this same temperature regime there appears a generally increased rotating frame rate $\Gamma_{1\rho}(D)$. If that increased rate also is quadrupolar, then we can conclude that $\Gamma_{1\rho q}$ is about $100\Gamma_{1q}$.

B. Niobium deuterides

The phase diagrams of the Nb-H and Nb-D systems are similar; no remarkable isotope differences having been reported between the two.[7] Like the Ta-D systems, the α or α' phase is an interstitial solid solution with a disordered deuterium occupancy in the tetrahedral sites of the bcc host metal lattice. The ordered deuterium arrangements have been determined by neutron diffraction.[23-25] The β phase based on the superstructure Nb-D isomorphic with δ-TaD is a tetrahedral MX-type superstructure. Within a range of concentrations close to $NbD_{0.50}$, i.e., $0.47 < X/M < 0.64$, the ζ phase in the Nb-D system shows the M_2X superstructure. In this phase deuterium resides on only one of the two interstitial tetrahedral sublattices occupied in β phase. The ϵ phase has M_4D_3 structure. The existence of ζ phase in the intermediate temperature range between β and ϵ phases has been identified by transmission electron microscope studies of Schober.[26]

$NbD_{0.55}$ spectra have a number of features in common with $TaD_{0.60}$ spectra. In the α and α' phases, rapid diffusion of deuterium among the bcc tetrahedral interstitial sites averages out the quadrupole interaction and produces a narrowed DMR line. At lower temperatures ($T < 200$ K), the β-phase signal is complex, with quadrupole structure which survives the hopping among restricted sites. Figure 7 shows the compound $(\alpha+\beta)$ spectra at 333 K (3.00) and 217 K (4.61). The quadrupole coupling parameters ν_q and η at 217 K are 45 kHz and 0.1, respectively. The spectrum (as in $TaD_{0.60}$) shows an asymmetry

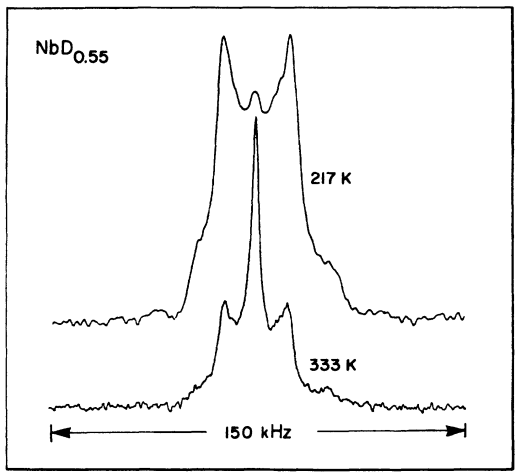

FIG. 7. DMR line shapes for $NbD_{0.55}$ in the $(\alpha+\beta)$ and $(\alpha+\zeta)$ phases at 333 and 217 K.

arising from a powder-averaged anisotropic Knight shift.[19] The β-phase ν_q and η are almost independent of deuterium concentration. As temperature decreases in the mixed $(\alpha+\beta)$ phase the center line characteristic of the α' phase diminishes while intensity from the satellites characteristic of the β phase grows. The transition α' to $(\alpha+\beta)$ occurs at 345 K (2.90) in $NbD_{0.55}$.

Spin-lattice relaxation in α' phase in both $NbD_{0.55}$ and $NbD_{0.88}$ exhibited two components which will be referred to as $\Gamma_{1s}(D)$ and $\Gamma_{1f}(D)$ corresponding to slow and fast decay rates, respectively. There is a good agreement between the $\Gamma_{1s}(D)$ results obtained in this work and the spin-lattice relaxation measurements of Lütgemeier, Bohn, and Arons[27] in a foil sample of $NbD_{0.36}$. A summary of the α'-phase two-component $T_1(D)$ results for $NbD_{0.55}$ and $NbD_{0.88}$ is shown in Fig. 8. The T_{1s} times for $NbD_{0.55}$ and $NbD_{0.88}$ (and those for $NbD_{0.36}$, not shown) show a crossover near 230 °C. This reversal occurs because the contribution of the conduction electrons to $\Gamma_{1s}(D)$ is larger in the less concentrated samples. The Korringa constant is smallest in $NbD_{0.36}$ and largest in $NbD_{0.88}$. The rapid changes of $T_1(D)$ at the cold side of Fig. 8 correspond to the transition to the $(\alpha+\beta)$ phase.

Results of three-parameter fits to the 7.55-MHz α'-phase $\Gamma_{1s}(D)$ in $NbD_{0.36}$, $NbD_{0.55}$, and $NbD_{0.88}$ are presented in Table II. Variation of these parameters with concentration is consistent with the observations in TaD_x and in niobium hydrides. Lütgemeier, Arons, and Bohn[28] estimate that $C_H \geq 300$ sec K in α-$NbH_{0.58}$ and $C_H \geq 650$ sec K in α-$NbH_{0.78}$. It follows that $C_D \geq 13000$ sec K in $NbD_{0.58}$ and $C_D \geq 28000$ sec K in $NbD_{0.78}$, in good agreement with the values listed in Table II. Dependence of C_D on concentration is shown in Fig. 2 and is identical to that observed in TaD_x.

Concentration dependence of the α-phase diffusion parameters has been investigated by Bauer, Vökl, Tretkowski, and Alefeld[15] in NbH_x and NbD_x $(x \leq 40\%)$ and by Williams[16] in NbH_x with $0.1 < x < 0.9$. Their activation energies E_H and E_D are plotted versus x in Fig. 9. Also shown are the ^2D activation energies obtained in the present work. The diamonds are from Gorsky-effect measurements[29,30] in NbH_x and the triangles[15] from NbD_x and NbH_x. E_H and E_D are heavily dependent on concentration for $x \leq 40\%$ and become constant at higher x. Diffusion measurements of the prefactor D_{0H} and D_{0D} of hydrogen and deuterium yield a large scatter without a clear isotope dependence of the sort which is well resolved in the activation energies data.

TABLE II. Reduced data from α'-NbD_x.

D/Nb	E_D (eV/atom)	$C_D = T_{1e}T$ (10^4 sec K)
0.36[a]	0.16 ± 0.015	0.65 ± 0.07
0.55	0.175 ± 0.015	1.3 ± 0.1
0.88	0.185 ± 0.010	3.3 ± 0.3

[a]Fit to the $\Gamma_1(D)$ of Lütgemeier *et al.* (Ref. 28).

The temperature variations of the variously measured α-phase $\Gamma_2(D)$ rates in NbD_x are similar to those in TaD_x. $\Gamma_2(D)$ as determined from linewidths, free-induction decays, and two-pulse echo envelopes are dominated by the magnetic and electric quadrupolar broadenings associated with bulk grain-size and dislocation effects. The corrected $\Gamma_2(D)$ deduced from zero time intercepts of rate versus τ^2 plots increase sharply near the $\alpha \rightarrow \alpha+\beta$ transition.

Figure 10 summarizes laboratory and rotating frame relaxation data for $NbD_{0.55}$ at 7.55 and 30.7 MHz. The $\Gamma_1(D)$ rates are independent of Larmor frequency in α' phase. In α' phase there is a small population $\Gamma_1(D)$ component with faster rates shown for 7.55 MHz by inverted triangles in Fig. 10. In the mixed $(\alpha+\beta)$ phase $\Gamma_1(D)$ was not measured for the α component and there the solid dots indicate rates $\Gamma_1(D)$ for the β component. There is little displacement of $\Gamma_1(D)$ in going from α' to $\alpha+\beta$ because the β-phase dipolar relaxation is about equal to the α'-phase quadrupolar rate. The vertical arrows indicate the reciprocal temperatures for the indicated DMR line shapes: 370 K (2.70), 333 K (3.00), and 217 K (4.61).

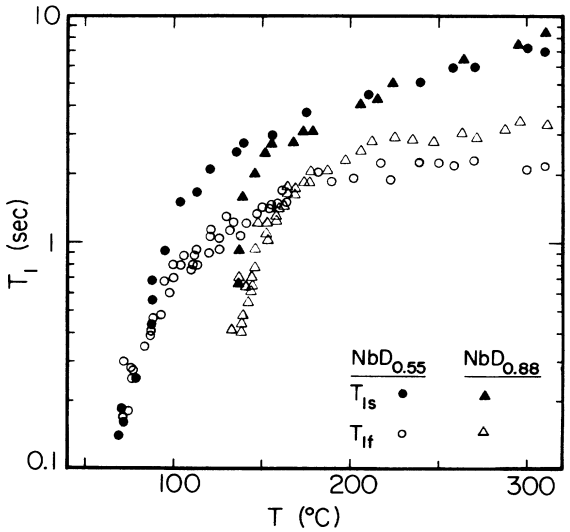

FIG. 8. Spin-lattice relaxation times $T_1(D)$ in $NbD_{0.55}$ (circles) and $NbD_{0.88}$ (triangles). Fast and slow relaxation components are shown.

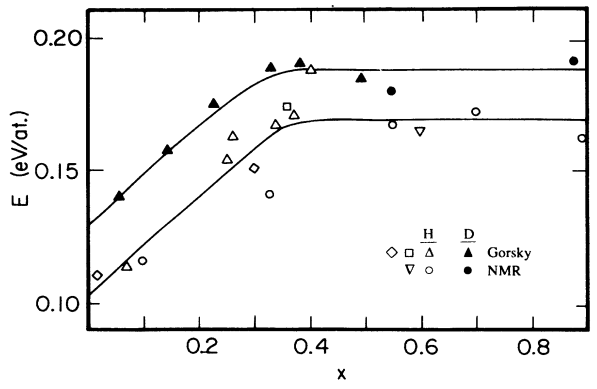

FIG. 9. Diffusional activation energies as a function of x in α-phase NbD_x and NbH_x. Gorsky effect and NMR determinations are shown (Refs. 15, 16, 29, and 30).

The vertical dashed lines indicate the reported $NbH_{0.55}$ phase transitions[7,23-26] between $(\alpha+\beta)$, $(\alpha+\zeta)$, and $(\alpha+\epsilon)$ phases. The vertical solid lines indicate the transitions $\alpha' \rightarrow (\alpha+\alpha')$ and $(\alpha+\alpha') \rightarrow (\alpha+\beta)$ in $NbD_{0.55}$.[31] It is possible that an $(\alpha+\alpha')$ phase in our $NbD_{0.55}$ sample accounts for the imperfectly steep increases in DMR rates near 2.80.

The dashed curve at the bottom of Fig. 10 shows the Γ_{1e} rate given in Table II for α-phase $NbD_{0.55}$. The two solid curves indicate dipolar deuteron rates Γ_{1d} scaled from proton NMR results. The lower curve is the 44.4-MHz $NbH_{0.58}$ proton rates of Lütgemeier, Arons, and Bohn[28] scaled by the γ^2 ratio of 42.44. The short dashed curve near the Γ_1 peak at $10^3/T=3.2$ shows the effect of a frequency correction 44.4/30.7 on these rates. The upper solid curve shows rates scaled by the γ^2 ratio from the 6.95-MHz $NbH_{0.55}$ results of Zamir and Cotts.[32] The motional dipolar relaxation peak at 6.95 MHz is less distorted by the phase changes near 345 K (2.90) since the peak occurs at lower temperature for the lower Larmor frequency. The short-dashed straight line to the left of the peak is drawn with the cold side slope and shows the distortional effect of the phase transitions. The sharp increase in the dipolar Γ_1 rate at the transition to the $(\alpha+\beta)$ phase reflects[30] the reduction of ω_c for hydrogen motion at the transition from cubic to orthorhombic structure.

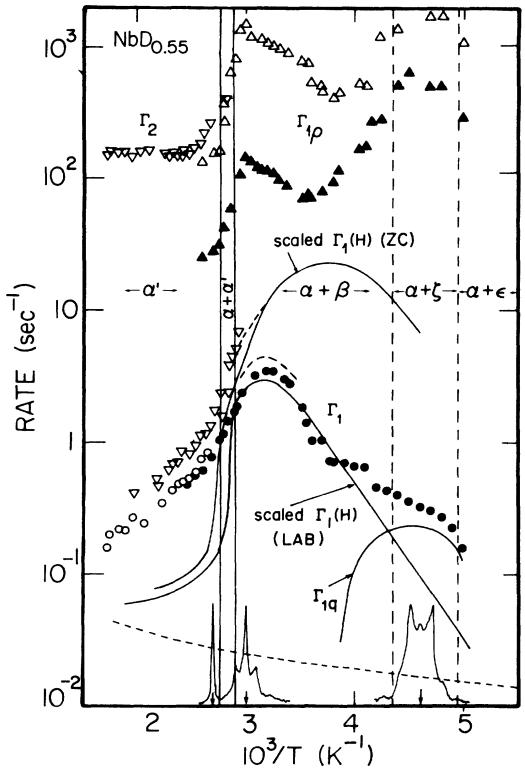

FIG. 10. Summary of DMR relaxation rates in $NbD_{0.55}$ between 200 and 578 K. As in TaD_x, Γ_1(D) in α phase is predominantly quadrupolar, but that in β phase is dipolar. Two solid curves show γ^2-scaled proton rates from Refs. 28 and 32. DMR spectra at the bottom correspond to the inverse temperatures indicated by arrows. Vertical lines indicate reported $NbH_{0.55}$ and $NbD_{0.55}$ phase changes (Refs. 7, 23–26, and 31).

Clearly the $(\alpha+\beta)$ mixed phase Γ_1(D) relaxation peak near $10^3/T=3.2$ is principally dipolar. Near a dipolar Γ_1(D) peak the rate in similar metal deuterides should scale as $\sqrt{\gamma(S(S+1))}$ for the metal nuclide (neglecting differences in M_e-D separations). For ^{93}Nb and ^{181}Ta this quantity scales as 2.56. The 30.7-MHz Γ_1(D) peak rates are 3.5 sec^{-1} (Nb, Fig. 10) and ≥ 1.35 sec^{-1} (Ta, Fig. 6), which correspond to a ratio ≤ 2.59. For $NbD_{0.55}$ the dipolar rate (solid line) lies below the cold sample rates for $10^3/T>4$ and the corresponding quadrupolar rate Γ_{1q} is indicated by the difference curve plotted.

At the top of Fig. 10 are plotted the fast and slow component spin lock rates $\Gamma_{1\rho f}$ and $\Gamma_{1\rho s}$. Between $10^3/T=3.0$ and 3.5, both show a decrease which has the same temperature dependence as does Γ_1(D)($E_{act}=0.22$ eV/atom). At lower temperatures near 250 K (4.00), where the laboratory frame quadrupolar rate Γ_{1q} contribution increases, there is a corresponding $\Gamma_{1\rho q}$ rate which is about $2350\Gamma_1$ for $\Gamma_{1\rho s}$ and $6500\Gamma_1$ for $\Gamma_{1\rho f}$. From 385 K (2.60) to 333 K (3.00) the principal $\Gamma_{1\rho}$(D) fraction is associated with the slower rate $\Gamma_{1\rho s}$ (solid triangles) and reflects α-phase deuterons. Below 250 K (4.00) the faster $\Gamma_{1\rho f}$ component (open triangles) is much the majority fraction and the slower rate $\Gamma_{1\rho s}$ has become hard to determine.

Lütgemeier and co-workers[27,28] have reported that in $NbH_{0.3}$ and $NbD_{0.36}$ both the H and D atoms jump at a frequency of about 10^8 sec^{-1} near room temperature, with activation energies of 0.2 and 0.3 eV for H and D, respectively. However, as they pointed out there are other measurements[32,33] which give jump frequencies an order of magnitude larger. Direct measurements of the self-diffusion coefficient of hydrogen in α-phase $NbH_{0.6}$ have been made by Zogal and Cotts[33] using the NMR pulsed-field gradient technique. They reported $D_0(H)=6.6\times10^{-4}$ cm^2/sec and $E_a(H)=0.165$ eV/atom. In α phase our three parameter fits to the 13-MHz Γ_1(D) in $NbD_{0.36}$ of Lütgemeier *et al.*[27] and to our 7.55-MHz Γ_1(D) in $NbD_{0.55}$ and $NbD_{0.88}$ yield 0.16, 0.175, and 0.185 eV/atom, respectively.

C. Vanadium deuterides

V-D systems are more complex than the other transition-metal deuterides in that both *T* and *O* interstitial sites are occupied with appreciable probabilities. The vanadium hydrides also show large isotope effects and the phase diagram of the V-D system[34] is quite different from that of the V-H system. The α' phase is a deuterium-disordered phase, in which most deuteriums are distributed randomly over tetrahedral sites of the bcc metal lattice. In this phase, about 10% of the interstitial atoms[35] occupy octahedral sites. In the β phase the deuterium atoms occupy mostly the octahedral sites. The crystal structure is monoclinic at composition V_2D for deuterium concentrations between $0.47<D/M<0.64$. Two deuterium atoms in the unit cell occupy octahedral sites. V_2D differs from Ta_2D and other superstructures in that deuterium atoms in V_2D are positioned in octahedral sites while at the same time, deuterium atoms in a disordered solid solution occupy mainly the tetrahedral interstitial sites. $VD_{0.59}$ shows α

and β phases in coexistence up to 386 K with the α phase remaining stable down to 230 K. An unusual feature of the ordering process in the V_2D lattice is the transition of interstitials from tetrahedral sites into octahedral sites which occurs when the temperature decreases below about 386 K. A small fraction (15%) of the deuteriums have been found in other positions in both structures. In β phase, the number of deuterium atoms in the tetrahedral sites decreases as the sample temperature decreases, and the population of octahedral occupancy approaches the total number of deuterium atoms.

Evidence for the existence of the ζ phase was reported[36] from differential thermal analysis (DTA) work. Arons, Bohn, and Lütgemeier[37] concluded that octahedral sites are occupied in the β phase, whereas the tetrahedral sites are dominant in the δ phase. Ordered structure of the δ phase was studied by neutron diffraction and shown to be isomorphic with β NbD. The δ phase exists at temperatures from 150 K to about 210 K. The structure of this partially ordered phase is orthorhombic with tetrahedral occupancy.

Figure 11 shows α' component DMR linewidths for $VD_{0.59}$ in the α' and mixed $(\alpha+\beta)$ phases. The squares indicate $\Gamma_2(D)$ determined as half-width at half maximum (HWHM) linewidths of Fourier-transformed 30-MHz echoes and include distortions from particle size effects. The solid dots indicate 7.55-MHz-corrected $\Gamma_{2t}(D)$ rates obtained from echo train envelopes extrapolated to $\tau=0$. The difference between the squares and dots is about 8×10^3 sec^{-1}. The triangles, crosses, and open circles indicate 30-MHz rotating-frame spin-lock rates $\Gamma_{1\rho}(D)$ at three rf H_1 fields: 1.5, 4.3, and 9.0 G. At 1.5 G the spin locking is ineffective and the rates approach the laboratory frame transverse rates $\Gamma_{2t}(D)$ (solid dots).

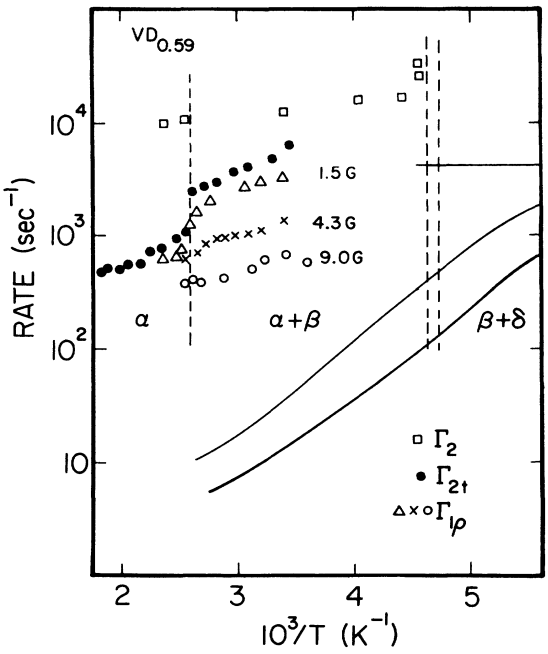

FIG. 11. Deuteron rates $\Gamma_2(D)$, $\Gamma_{2t}(D)$, and $\Gamma_{1\rho}(D)$ for $VD_{0.59}$ in the α' and mixed $(\alpha+\beta)$ phases. The solid curves and line indicate γ^2-scaled proton rates from the fast and slow $\Gamma_2(H)$ data of Hayashi *et al.* (Ref. 38) in $VH_{0.59}$. Dashed lines indicate reported $VD_{0.59}$ phase changes.

At the bottom of Fig. 11 the two solid curves indicate anticipated dipolar rates $\Gamma_{2d}(D)$, scaled by the γ^2 ratio (42.44) from the fast and slow proton echo $\Gamma_2(H)$ components at 55 MHz reported by Hayashi, Hayamizu, and Yamamoto[38] in $VH_{0.59}$. We conclude that most of our $\Gamma_{2t}(D)$ rate (solid dots) arises from quadrupolar broadenings. There is no evidence of any appreciable (nearly temperature independent) broadening from the anisotropic Knight shift.

In low-temperature phases a majority of deuteriums are known to occupy octahedral interstices lying between vanadium atoms on the c axis (O_z sites). The phases differ from each other in the arrangement of deuteriums within the interstitial sublattice of (O_z sites). It tends to cost less energy to place an atom on vacant O_z sites than on any other site. According to their model proposed by Asano, Abe, and Hirabayashi[39] the structures of these sites are characterized by the stacking sequences of two groups of 101 planes of (O_z sites), namely O_{z1} and O_{z2}. For a stoichiometric composition of $VD_{0.50}$, O_{z1} sites are filled with deuteriums, and O_{z2} sites are empty. O_{z2} planes become partially populated as more deuterium atoms are added.

Hayashi, Hayamizu, and Yamamoto[40] interpreted their two-component proton relaxation times $T_1(H)$ and $T_2(H)$ as a resolution of O_{z1} and O_{z2} fractions between 120 and 350 K. The ratio of magnetizations was temperature dependent with the broader component collapsing into the narrower one above 220 K as motional narrowing increased. Zogal and Stalinski have reported[41] similar results. For $VD_{0.59}$ most of the β-phase D occupy O_{z1} sites at lower temperatures and transfer gradually to the O_{z2} sites as the temperature increases. In the course of hopping a D spends different times on three types of sites; O_{z1}, O_{z2}, and T sites.

Figures 12 and 13 show 30.7-MHz Fourier-transformed DMR spectra in $VD_{0.59}$ at three temperatures. Figure 12 shows a motionally narrowed line at 390 K (2.56) in α phase, just above the phase transition $(\alpha+\beta)\rightarrow\alpha$. The spectrum has been taken 130 msec after inversion of the

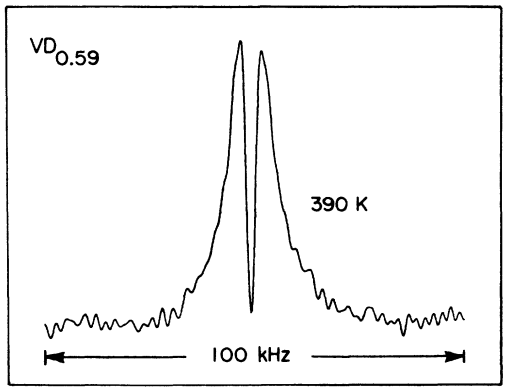

FIG. 12. A DMR spectrum in α-phase $VD_{0.59}$ at 390 K. The spectrum is partially recovered, following inversion of the entire line and shows compound spin-lattice relaxation with the broader line relaxing more rapidly than the narrower line.

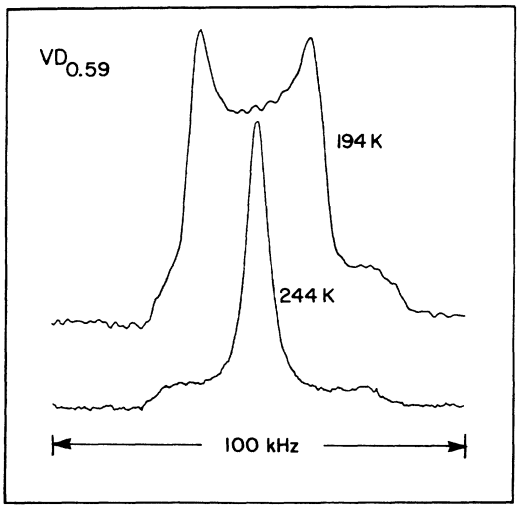

FIG. 13. DMR line shapes for $VD_{0.59}$ in the $(\alpha+\beta)$ and $(\beta+\delta)$ phases at 244 and 194 K. The β-component 53-kHz quadrupolar doublet singularities are barely discernible, while at 194 K, the narrower δ-phase 54-kHz splitting is clear. The α-phase component remains intense at 244 K. Effects of the anisotropic Knight shift are particularly evident at 194 K.

entire line by a 180° pulse. The narrowed line clearly is composite, with at least two distinct spin-lattice relaxation rates Γ_1. The broader component (6.4 kHz HWHM) has recovered appreciably towards its equilibrium magnetization while the narrower line (1.6 kHz HWHM) still is inverted and has a slower Γ_1 rate (0.82 sec^{-1} compared to 2.1 sec^{-1}). It is probable that the more narrow line with slower Γ_1 corresponds to D hopping among T sites, while the broader and faster-relaxing wings of the line correspond to hopping among O sites.

A mixture of two quadrupole-split spectra and a single unsplit broad line has been reported in the $(\beta+\delta)$ and $(\beta+\zeta)$ range of 200 to 220 K. Arons, Bohn, and Lütgemeier[37] and Roenker[2] examined VD_x with x between 0.5 and 0.6 and found a triple point with α, β, and δ phases in coexistence at about 210 and 205 K, respectively. Arons *et al.* concluded that in β phase the quadrupolar doublet corresponded to $\nu_Q = 105$ kHz up to about 210 K, decreasing to 100 kHz near 300 K and 90 kHz by 410 K. In δ phase the doublet corresponded to $\nu_Q = 55$ kHz up to about 210 K and then decreased to about 48 kHz at 226 K in $VD_{0.62}$. Deuteriums occupy mostly octahedral O sites in β phase and mostly tetrahedral T sites in δ (and α) phase. In both O and T sites the electric field gradient has its largest component parallel to a cube edge. The relative intensities of the two quadrupole-split spectra varied with temperature.

Figure 13 shows a 30.7-MHz DMR spectrum for $VD_{0.59}$ in the $(\alpha+\beta)$ mixed phase at 244 K (4.10). Even at this low temperature the α-phase narrow component remains more intense than the β-phase base pedestal spectrum with its barely discernible peaks near a 53-kHz splitting ($\nu_q = 106$ kHz). Figure 13 also shows a DMR spectrum at 194 K (5.15) in the $(\beta+\delta)$ mixed phase. The α component has vanished, as has any clear β doublet. Instead there is a δ-phase doublet spectrum with main peak separation 27 kHz ($\nu_q \simeq 54$ kHz) and distorted[19] by a significant anisotropic Knight shift. The asymmetry parameter η is $\simeq 0.1$.

In our measurements $VD_{0.59}$ displayed compound DMR relaxation times at all temperatures studied. Figures 14 and 15 summarize the temperature variations of the fast and slow components of $\Gamma_1(D)$ and spin-lock $\Gamma_{1\rho}(D)$. The full vertical lines indicate the reported[7] phase transitions for $VD_{0.59}$ $\alpha \rightarrow (\alpha+\beta) \rightarrow (\beta+\zeta) \rightarrow (\beta+\delta)$ at 386 K (2.59), 217 K (4.60), and 212 K (4.72). At the bottom of Figs. 14 and 15 three small spectra show the DMR line shapes at the temperatures indicated by the arrows at 420, 244, and 194 K. The latter two spectra are from Figs. 13.

The dashed curve near the bottom of Figs. 14 and 15 indicates the electron relaxation contribution $\Gamma_{1e}(D)$ determined from our α-phase analysis and γ^2 scaled from the proton data of Kazama and Fukai.[42] The dashed peak above this indicates γ^2 scaling of the relaxation rates $\Gamma_1(H)$ observed by Fukai and Kazama[43] at 5.0 MHz and interpolated to $VH_{0.59}$ from their data at $x = 0.546$ and 0.622. The dual dipolar $\Gamma_1(H)$ peaks have been interpreted as being associated with hopping among T sites (3.25) and among O sites (4.75). The compound spectrum of Fig. 12 at 390 K (2.56) corresponds to the $\Gamma_1(D)$ rates (0.81 and 2.1 sec^{-1}) indicated by the first solid circles on

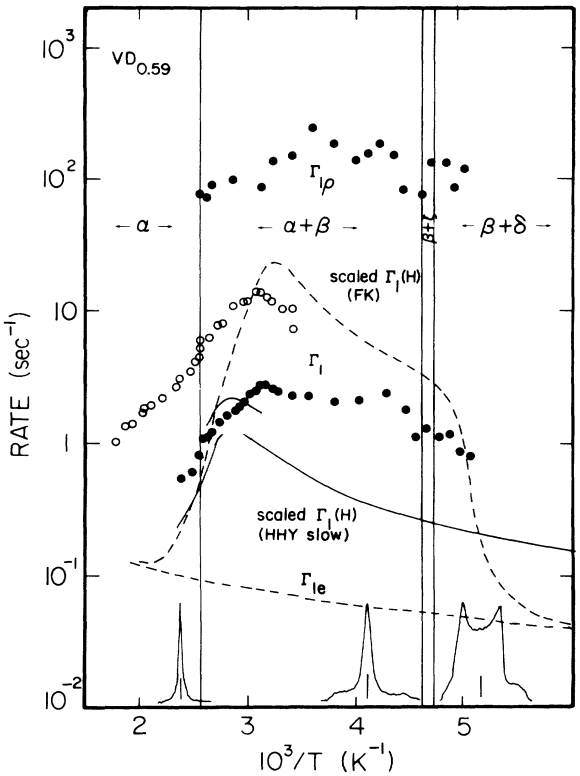

FIG. 14. Fast component $\Gamma_1(D)$ and $\Gamma_{1\rho}(D)$ rates for $VD_{0.59}$. Open circles are 7.55-MHz rates and solid dots are 30.7-MHz results. Deuteron rates are compared with scaled protons rates given by dashed and solid peaks. DMR spectra occur as indicated. There is a distinct quadrupolar peak in $\Gamma_1(D)$ and $\Gamma_{1\rho}(D)$ at lower temperatures.

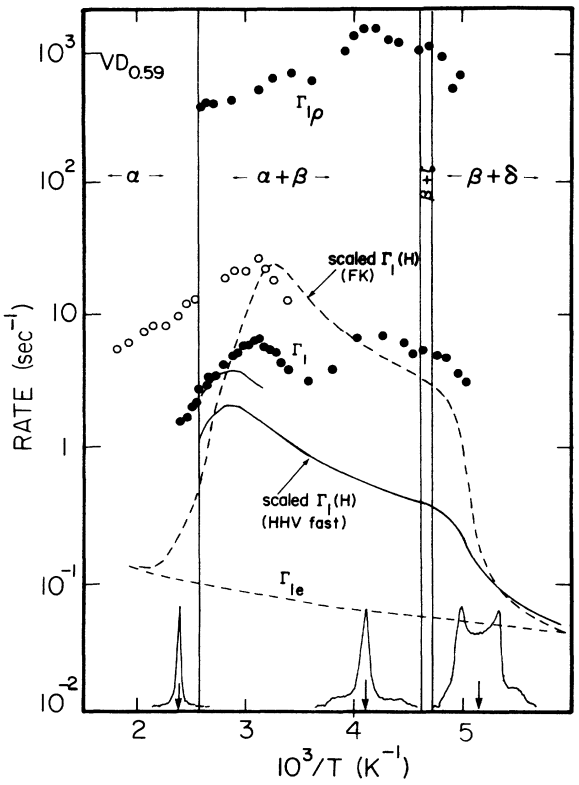

FIG. 15. Slow component Γ_1(D) and $\Gamma_{1\rho}$(D) rates for $VD_{0.59}$. Open circles are 7.55-MHz rates and solid dots are 30.7-MHz results.

the warm side of the $\alpha \rightarrow (\alpha+\beta)$ transition.

Hayashi, Hayamizu, and Yamamoto[40] have reported two-component fast and slow Γ_1(H) rates for protons in $VH_{0.59}$. The solid curves in Figs. 14 and 15 show these rates, scaled down by the γ^2 factor of 42.44. In both figures a short solid curve near the principal Γ_1 peak shows the Γ_1(H) rates also scaled by a linear frequency factor (55/30.7). These reflect peak deuteron dipolar rates Γ_{1d}(D) if the substantial isotopic variations in phase diagram and hydrogen hopping are neglected, along with H-H dipolar interactions.

In Figs. 14 and 15 the lower sets of solid dots indicate the fast and slow Γ_1(D) spin-lattice rates observed at 30.7 MHz in the present work. Above these the open circles similarly indicate the fast and slow Γ_1(D) components at 7.55 MHz. At the top of the figures the solid circles indicate the fast and slow 30.7-MHz spin-lock rates $\Gamma_{1\rho}$(D) observed in the rotating frame at 9 G H_1.

To a first approximation the fast and slow Γ_1(D) [and $\Gamma_{1\rho}$(D)] rates differ by about a factor of 2. At 7.55 MHz the slow Γ_1(D) component corresponds to about 60% of the spins from 556 K (1.80) to 294 K (3.40). However, at 30.7 MHz the slow Γ_1(D) component corresponds to only some 20% of the spins at 389 K (2.57). This slow fraction increases to 60% at 308 K (3.25) and then decreases again below 250 K (4.00) to 50% at 222 K (4.50) and below. It is probable that the 30.7-MHz measurements included more of the broad-line spectral components than did the 7.55-MHz measurements. Presumably in α' phase the slow Γ_1(D), narrower line fraction reflects D hopping with the majority T-site occupancy.

To the extent that the solid curve peaks near 2.90 accurately reflect dipolar rates Γ_{1d}(D), it is clear that the solid-circle peak Γ_1(D) rates are primarily, but not entirely dipolar. There is an $\simeq$30% quadrupolar relaxation near the 3.15 Γ_1(D) peaks, a pattern quite different from that in $TaD_{0.60}$ and $NbD_{0.55}$.

The quadrupolar relaxation which becomes totally dominant in α phase is not extreme narrowed since it displays a linear ω_0 dependence between the 30.7- and 7.55-MHz Γ_1(D) rates. Here the D hopping rates are larger than ω_0, so the absence of extreme narrowing $\omega 0$-independent relaxation indicates that even in the α' phase there is some restricted hopping among a partially ordered subset of D sites. The complex spectrum of Fig. 12 supports this view.

IV. CONCLUSIONS

Dipolar γ^2 scaling, which can be misleading in comparing metal hydride and metal deuteride results for fcc structures, works very well in the bcc transition-metal deuterides of Ta, Nb, and V. It permits rather confident identification of nuclear relaxation rates arising from conduction electrons, from nuclear dipolar interactions, and from nuclear quadrupolar interactions.

In all the samples studied, rapid deuteron hopping among ordered sites in the warm β phase not only does not average out the structured quadrupolar line shape but also produces no effective quadrupolar spin-lattice relaxation in the laboratory frame. The hopping among a restricted subset of sites in the distorted β phase produces a predominantly dipolar Γ_1 rate. As non-β phases appear at lower temperatures, quadrupolar relaxation reappears in both laboratory and rotating frames, especially in those temperature regimes where proton relaxations have been interpreted to reflect hopping among O sites.

In TaD_x and NbD_x the α-phase deuteron relaxations are in the extreme-narrowed regime, with the quadrupolar Γ_{1q}(D) independent of ω_0. From the relaxation rates we infer diffusional activation energies systematically greater than those for corresponding hydrides, but with similar dependence on hydrogen concentration. The electron-induced rates Γ_{1e}(D) and the Korringa constant C scale as γ^2. For Ta and Nb we find that $C(\text{Nb}) = C(\text{Ta})$. In β phase the deuteron hopping rate is larger in Nb than in Ta, since at the $(\alpha+\beta) \rightarrow \alpha$ transition in Ta the Γ_1(D) relaxation has not yet reached its peak rate, contrary to the Nb results in the same temperature range.

$VD_{0.59}$ presents complications in addition to those anticipated from joint T- and O-site deuteron occupancy. In α phase the Γ_1(D) relaxations show two clear component rates and each of these fast and slow rates exhibits an apparent ω_0 dependence. Since the hopping rates are fast compared to ω_0, some partial hopping among ordered sites must persist into the α phase. Further measurements are needed on this topic.

Since dipolar relaxation plays such a small role in α-phase relaxation in all the samples studied, it has not been necessary to take account of the corrections[14-44] arising from site occupancy. The precision of γ^2 scaling of $\Gamma_1(H)$ rates in Ta and Nb samples supports the proposal of excluded nearest-neighbor proton occupancy. There is little H-H dipolar $\Gamma_1(H)$ relaxation. Thus it is not necessary to employ the proposed[27] 1.5 multiplicative factor in γ^2 scaling.

ACKNOWLEDGMENTS

The metal deuteride samples were provided by R. G. Barnes at Iowa State University. We have benefited from discussions with M. S. Conradi, R. M. Cotts, P. A. Fedders, and R. K. Sundfors. This work was supported in part by the national Science Foundation division of Materials Research under Grant No. DMR 85-03083 and its predecessor Grant No. DMR 82-04166.

*Present address: Department of Physics, University of Nevada, Reno, NE 89557.

†Present address: Varian Associates, Palo Alto, CA 94089.

‡Permanent address: Department of Physics, Principia College, Elsah, IL 62028.

[1]E. F. W. Seymour, J. Less Common Met. **88**, 323 (1982).

[2]K. P. Roenker, Ph.D. thesis, Iowa State University, 1973.

[3]D. Slotfeld-Ellingsen and B. Pedersen, Phys. Status Solidi (a) **25**, 115 (1974).

[4]E. L. Hahn, Phys. Rev. **80**, 580 (1950).

[5]S. Meiboom and D. Gill, Rev. Sci. Instrum. **29**, 688 (1958).

[6]R. C. Wayne, D. Zamir, and J. H. Strange, Rev. Sci. Instrum. **35**, 1051 (1964).

[7]T. Schober and H. Wenzl, in *Hydrogen in Metals II,* edited by G. Alefeld and J. Völkl (Springer, Berlin, 1978), p. 11.

[8]U. Köbler and T. Schober, J. Less Common Met. **60**, 101 (1978).

[9]H. Asano, Y. Ishino, R. Yamada, and M. Hirabayashi, J. Solid State Chem. **15**, 45 (1975).

[10]H. T. Weaver, J. Magn. Reson. **15**, 84 (1974).

[11]J. Korringa, Physica **16**, 601 (1950).

[12]Shigeo Kazama and Yuh Fukai, in *Proceedings of JIMIS-2* [Hydrogen Met. **173**, (1980)].

[13]N. Bloembergen, E. M. Purcell, and R. V. Pound, Phys. Rev. **73**, 679 (1948).

[14]P. E. Mauger, W. D. Williams, and R. M. Cotts, J. Phys. Chem. Solids **42**, 821 (1981).

[15]H. C. Bauer, J. Vökl, J. Tretkowski, and G. Alefeld, Z. Phys. B **29**, 19 (1978).

[16]W. D. Williams, Ph.D. thesis, Cornell University, 1976.

[17]R. M. Cotts (private communication).

[18]D. Zamir and R. M. Cotts, Phys. Rev. **134**, A666 (1964).

[19]D. R. Torgeson, R. J. Schoenberger, and R. G. Barnes, Bull. Am. Phys. Soc. **31**, 270 (1986).

[20]P. A. Hornung, Ph.D. thesis, Iowa State University, 1978.

[21]S. Kazama, Y. Fukai, J. Less Common Met. **53**, 25 (1977).

[22]P. A. Hornung, A. D. Khan, D. R. Torgeson, and R. G. Barnes Z. Phys. Chem. **116**, 77 (1979).

[23]V. A. Somenkov, A. V. Guerskaya, M. G. Zemlyanov, M. E. Kost, N. A. Chernoplekov, and A. A. Chertkov, Fiz. Tverd. Tela **10**, 1355 (1968) [Sov. Phys. Solid State **10**, 1076 (1968)].

[24]V. A. Somenkov, V. F. Petrunin, S. Sh. Shil'stein, and A. A. Chertkol, Kristallografiya **15**, 601 (1970) [Sov. Phys. Crystallogr. **14**, 522 (1970)].

[25]V. A. Somenkov, Ber. Bunsenges. Phys. Chem. **76**, 733 (1972).

[26]T. Schober, Scr. Metall. **7**, 1119 (1973).

[27]H. Lütgemeier, H. G. Bohn, and R. R. Arons, J. Magn. Reson. **8**, 80 (1972).

[28]H. Lütgemeier, R. R. Arons, H. G. Bohn, J. Magn. Reson. **8**, 74 (1972).

[29]G. Schaumann, J. Vökl, and G. Alefeld, Phys. Status Solidi **42**, 401 (1970).

[30]J. Tretkowski, J. Vökl, and G. Alefeld, Z. Naturforsch. **26a**, 588 (1971).

[31]R. J. Walter and W. T. Chandler, Trans. AIME **233**, 762 (1965).

[32]D. Zamir and R. M. Cotts, Phys. Rev. **134**, A666 (1964).

[33]O. J. Zogal and R. M. Cotts, Phys. Rev. B **11**, 2443 (1975).

[34]T. Schober and A. Carl, Phys. Status Solidi (a) **43**, 443 (1977).

[35]V. A. Somenkov *et al.* Fiz. Tverd. Tela **13**, 2595 (1971) [Sov. Phys. Solid State **13**, 2178 (1972)].

[36]T. Schober and W. Pesch, Z. Phys. Chem. **B114b**, 521 (1979).

[37]R. R. Arons, H. G. Bohn, and H. Lütgemeier, J. Phys. Chem. Solids **35**, 207 (1974).

[38]S. Hayashi, K. Hayamizu, and O. Yamamoto, Solid State Commun. **41**, 743 (1982).

[39]H. Asano, Y. Abe, and M. Hirabayashi, J. Phys. Soc. Jpn. **41**, 974 (1976).

[40]S. Hayashi, K. Hayamizu, and O. Yamamoto, J. Chem. Phys. **76**, 4392 (1982).

[41]O. J. Zogal and B. Stalinski, in *Proceedings of the International Conference on Magnetic Resonance and Relaxation, Fourteenth Colloque Ampère, Ljubljana, Yugoslavia, 1966,* edited by R. Blinc (North-Holland, Amsterdam, 1968).

[42]S. Kazama and Y. Fakai, J. Phys. Soc. Jpn. **42**, 119 (1977).

[43]Y. Fukai and S. Kazama, Acta Metall. **25**, 59 (1977).

[44]P. A. Fedders and O. F. Sankey, Phys. Rev. B **18**, 5938 (1978); **20**, 39 (1979).